Chapter 7

Case studies

In Chapter 6, two different field methods such as thermal response tests (TRTs) and short-term thermal tracer tests (TTTs) for the investigation of closed and open geothermal systems were discussed. Here the focus is on **long-term injection-storage and recovery experiments** and **regional studies on thermal use**.

The experiment on **aquifer storage and recovery of heated water** by Molz et al. (1978) at the **Auburn site near Mobile** (Alabama, USA) was numerically simulated and compared with field data by Papadopulos and Larson (1978). The results confirmed the utility of the simulation tools. Based on their analysis, the experimental techniques were improved by Molz et al. (1981) and successfully modeled by Tsang et al. (1981). The experiment consisted of the injection of 55,000 m^3 of water of a temperature of 55.2°C into the aquifer of ambient temperature of 20°C. An injection period of 79 days was followed by a recovery phase of 52 days. The simulated production temperature of 32.8°C and the recovery rate (66%) agreed well with the observations. Parr et al. (1983) performed a field determination of the thermal energy storage parameters for the Mobile aquifer. Geochemical, thermal, and hydrogeological parameters were estimated by laboratory and field studies for the aquifer and the confining layers. The investigated parameters were the regional flow gradient, the vertical and horizontal hydraulic conductivities of the aquifer, the horizontal dispersivity, the vertical hydraulic conductivity of the confining layers, the thermal conductivities, heat capacities, and chemical characteristics of the aquifer matrix, and the groundwater.

Sauty et al. (1982b) performed field experiments of **warm water storage in a sandy gravel aquifer** confined by clay layers at the **Bonnaud** (Jura) site (France). The injected water volumes ranged from 500 to 1700 m^3. The injection temperature ranged between 32.5°C and 40°C. Temperature profiles were observed in 17 boreholes. The results were discussed and were used to calibrate two mathematical models. A two-dimensional axisymmetric finite difference code (Sauty et al. 1982a) was used to determine the mean values of the parameters thermal conductivity, heat capacity, and thermal

dispersivity of four layers (Table 6.2). A three-dimensional finite difference model was used to determine their spatial variations in the horizontal plane. In both models, density effects were disregarded. Finally, the results of the storage experiments were successfully compared with the general type curves for the production temperature, which were developed by Sauty et al. (1982a).

Kobus and Söll (1992) modeled regional heat transport for two case studies in the shallow, unconfined, sandy gravel **Emme aquifer** close to **Kirchberg** (Switzerland). The first case study concerned the injection of cold water at the **Aefligen** (Switzerland) site (Blau et al. 1991). The test consisted of **local infiltration** of 2 m^3 min^{-1}, at a temperature between 2°C and 7°C, in an intermittent manner over a period of 150 days. The average infiltration rate was 2 m^3 min^{-1}. The thermal plume was observed in several boreholes. It was simulated by Söll (1985) with the support of a transient vertical model along streamlines. With detailed consideration of the vertical velocity distribution and neglecting thermal dispersion, the comparison with field data was satisfactory. However, when using depth-averaged velocities, thermal macrodispersion effects, depending on the flow distance, were important. The second case study was the **natural river water infiltration** from the river Emme into the aquifer near Kirchberg (Blau et al. 1991). For the horizontal modeling, two aquifer layers were necessary since a single depth-averaged aquifer model was not able to account for the different flow directions in both layers. The soil layer and the underlying impermeable layer were taken into account by analytical solutions for the heat flux.

Thermal energy storage in an unconfined sand aquifer at the **Borden site** (Canada) was investigated by Palmer et al. (1992). Heated water was injected into a shallow aquifer, and thermal plume temperature was monitored in a dense array of piezometers. The total water volume of 53.5 m^3 of temperature 35°C (with fluctuations between 34°C and 39°C) was injected within 6 days. The initial temperature ranged between 9.5°C (at depth 6.1 m) and 15°C (depth 0.5 m). The detailed monitoring provided the three-dimensional temperature distribution within the aquifer. The data were used by Molson et al. (1992) to develop and validate a three-dimensional coupled, density-dependent numerical model. The simulations provided an excellent match between observations and the model. Thermal input parameters, such as thermal dispersivity values, were obtained from either literature data or from data analysis (Table 6.2).

Xue et al. (1990) performed simulations for three **seasonal aquifer thermal energy storage** experiments conducted in **Shanghai** (China). They used a three-dimensional flow and heat transport model. The aquifer used for the heat storage was a confined sand formation. The results (temperature and recovery rates) agreed well with the observations. They showed that heat dispersion was important.

Birkholzer and Zhang (2000) modeled **hydrologic and thermal processes in a large-scale underground heater test in partially saturated fractured tuff at the Yucca Mountain site** (USA). They used the code TOUGH2 to simulate coupled water, water vapor, air, and heat transport in unsaturated fractured porous media. The agreement of the model results with long-term measurements indicated that the understanding of the complex process was satisfactory.

Markle et al. (2006) developed a **method for constructing the two-dimensional vertical thermal conductivity field** for a 12 m (horizontal) × 8 m (vertical) section of a glaciofluvial sand and gravel outwash deposit (**Tricks Creek study area**) in southwestern Ontario, Canada. The method used both field and laboratory measurements to determine the bulk thermal conductivity of the aquifer solids, the volumetric water content, and the porosity of the aquifer. Based on a model selection procedure using the information-theory approach, the Campbell model (Chapter 2.1.2.2) was selected as approximating the apparent thermal conductivity of variably saturated sands and gravels best. Thermal conductivities of the solid material of the aquifer were determined using two laboratory methods, first using the so-called divided-bar apparatus (Sass et al. 1971) and second using the mineral composition of the aquifer material. The mean thermal conductivity of fine to coarse sand was 4.22 ± 0.10 W m^{-1} K^{-1}, for gravel and sand it was 3.94 ± 0.12 W m^{-1} K^{-1}, and for till 3.72 ± 0.59 W m^{-1} K^{-1}. The two-dimensional vertical apparent thermal conductivity field was obtained by combining measured thermal conductivities and site stratigraphy with the measured porosity values. The resulting thermal conductivity field was used as input to a transient numerical model for simulating heat transport. In the saturated zone, the mean value and standard deviation of apparent thermal conductivity were 2.42 and 0.13 W m^{-1} K^{-1}, respectively. The apparent thermal conductivities in the unsaturated zone were between 40% and 50% lower than the apparent thermal conductivities in the saturated zone. Porosity strongly influenced the predicted two-dimensional conductivity field, indicating that this parameter has to be defined carefully. Numerical simulations were performed using the finite element numerical model HEATFLOW (Molson et al. 1992) after modifications were made to include the Campbell model for apparent thermal conductivity. Density effects on flow were taken into account. Numerical simulations were performed for a transport time of 10 days for both heterogeneous and average thermal conductivity fields. In both cases, uniform hydraulic conductivity was assumed. The simulations showed that using a homogeneous thermal conductivity instead of a fully heterogeneous field would yield temperature differences of less than 1 K relative to the heterogeneous cases. The authors concluded that, whenever small temperature differences are important, consideration of the heterogeneities in thermal conductivity may be necessary.

Lo Russo and Civita (2009) performed numerical investigations using FEFLOW for open-loop heat pumps of a **field study near Torino** (Italy). They tested scenarios with respect to the environmental impact.

Nam and Ooka (2010) performed numerical heat transfer simulations for their case study at the **Chiba experimental station** in Tokyo (Japan). The simulation model was confirmed by the experimental results. Based on the model, several methods for achieving an optimal coefficient of performance were tested.

Kupfersberger (2009) investigated the **impact of groundwater heat pumps** in the shallow sandy gravel aquifer Leibnitzer Feld (Leibnitz close to Graz, Austria) with the help of a two-dimensional numerical flow and heat transport model using the FEFLOW software. Transient head data were used to calibrate the flow model. A heat-transfer function between soil surface (using air temperature) and groundwater was established to represent the heat input rate. The heat transfer coefficients (transfer-in and transfer-out parameters) were calibrated using observed temperature profiles. The temperature of the reinjected water was limited to a decrease of 5 K and an absolute minimum of 5°C by Austrian law. The limited temperature fluctuations justified neglecting density effects in the flow modeling. The annual heat extractions of three users were assumed to be 116, 321, and 600 MWh, respectively. It was shown that the reduction of the groundwater temperature 300 m downstream of the reinjection wells was less than 0.5°C in these cases, hence demonstrating the feasibility and potential of the thermal use.

Vandenbohede et al. (2011) studied the heat transport during a **shallow heat injection and storage field test at the Ghent University site** in Ghent (Belgium). The seasonal temperature fluctuations were simulated using the code SEAWAT. They found that the most sensitive parameter is the thermal conductivity of the solid phase followed by the porosity, the heat capacity of the solid, and the longitudinal dispersivity. They demonstrated the dominance of conductive transport during the storage phase, while the convective transport was dominant during the injection phase. They concluded that dispersivity cannot be ignored in the simulation of advective heat transport in aquifers.

In the following, two regional case studies from Austria and Switzerland and one local case study of a ground source heat pump system in Germany are presented in more details.

7.1 CASE STUDY ALTACH (AUSTRIA)

The **change of the thermal regime due to the thermal use of the aquifer in the Rhine valley in the region of Altach in the State of Vorarlberg** (Austria) was investigated using a two-dimensional numerical model (Cathomen

2002; Cathomen et al. 2002). The task consisted of evaluating the impact of existing installations of open systems with and without heat pumps and the warming effects of buildings (warm basements) on the groundwater temperature. The motivation was to compare long-term effects with local temperature measurements in order to assess a possible overexploitation of the thermal resource. In the State of Vorarlberg, the thermal use of aquifers using heat pumps has been promoted and supported since the 1980s. For this purpose, the thermal potential of the regional aquifer was assessed by the State authorities, with the help of a water and heat balance over subregions. Based on these investigations, licenses for thermal use have been issued by the authorities. In those times, the State of Vorarlberg limited the allowed maximum change of the temperature in aquifers to 1 K. Since measurements indicated that the maximum temperature decrease reached about 1 K locally, the question of whether the maximum potential is already exhausted arose. However, meanwhile, the authorities of Austria fixed the maximum allowable change to 6 K, relative to the existing groundwater temperature at the location of the reinjection (ÖWAV 2009; Chapter 1.8.2). Thus, the situation is uncritical now.

The **town and the region of Altach** are located about 20 km south of Bregenz, the capital of the State of Vorarlberg, within the **plain of the Rhine valley** at an altitude of 412 m a.s.l. The **boundaries of the investigation area** were chosen such that no thermal plumes from neighboring regions were included. The resulting domain was about 21 km^2 in size. It was delimited at the western boundary by River Rhine (flowing from southwest to northeast) and Alter Rhein, which is an oxbow lake of the old course of the river. The northeastern and the southern boundaries were chosen along steady-state streamlines. The northeastern boundary as well as part of the southwestern boundary delimit the highly permeable region, which borders hilly and mountainous regions. The domain contains eight groundwater pumping stations and several creeks. The **annual mean air temperature** (2 m above soil surface) is 10.1°C, and the **mean temperature of the soil surface** (in 5 cm depth) is about 11.2°C. These data were measured in 1999 at the meteorological station of Vaduz (Principality of Liechtenstein), which is located about 30 km south of Altach up-valley at an altitude of 460 m a.s.l., and which is run by MeteoSwiss. In 1999, precipitation was 1297 mm. The average temperature of River Rhine (Hydrological Annual Book of Switzerland, 2000, station Diepoldsau) was 8.1°C in the year 2000 and therefore cooler than air and soil surface temperature (7.8°C in the period 1984–2000). However, since groundwater is essentially outflowing into River Rhine, only limited cooling effects are expected.

Geologically, the Rhine valley is essentially filled with unconsolidated rock material, which was deposited into an elongated lake during the last ice age. Fine-grained sediments form the bottom of a sandy gravel aquifer, which represents the highly conductive top layer. The aquifer thickness is

typically 15–20 m, and the depth to groundwater is 2–4 m. Hydraulic conductivity values are on the order of 2×10^{-3} m s^{-1}. Furthermore, two large alluvial cones were deposited by creeks from hills and mountains. In these subregions, the altitude and thus the depth to groundwater are increased accordingly.

The domain contains the **communities and towns of Altach, Mäder, and Hohenems** with a total population of about 30,000 inhabitants. Land use in the region is mainly agriculture (about 50% of the area) and settlements as well as industry. Data of the State of Vorarlberg allowed a quantification of the thermal input and extractions (Table 7.1). A total of 323 (2002) **installations with groundwater heat pump systems** with a total annual mean performance of 1.35 MW was registered. Concerning the groundwater temperature, the Hydrographic Service of the State of Vorarlberg performed **periodic or permanent temperature measurements** in several boreholes. These measurements were taken routinely at a fixed depth of 1 m below the lowest expected groundwater table. The annual mean groundwater temperature of five stations was 11.5°C with mean values at the individual stations between 10.4°C and 11.9°C. These data were complemented by the **measurement of temperature profiles** in a total of 17 piezometers within the domain, with the help of the Hydrographic Service (Figure 7.1). The temperature profiles were measured in late fall (November 13, 2001) using a thermal borehole probe, in intervals of 1 m, starting at the water table. Most of the temperature profiles follow the characteristic shape of a damped harmonic wave according to Equation 3.85 for one-dimensional vertical conductive heat transport for this date. The maximum temperature was observed at a depth of about 4–5 m below soil surface. Most of the profiles tend toward the annual mean temperature of approximately 11°C at a depth of about 10 m. Exceptions are stations 50.4.07 and Kropf-2. The former profile was possibly influenced by vertical flow in the borehole, with inflowing groundwater at larger depths into and outflowing groundwater at higher depths out of the borehole. The piezometer of the latter profile is situated close to a groundwater lake (formed by gravel exploitation) with stagnant water, which can possibly influence the groundwater temperature. The variability of the rest of the temperature profiles can be attributed to local land use and the thermal properties of the local material, but also by the thermal use of the aquifer.

Table 7.1 Altach study: annual total heat flux

Thermal input category	*Thermal input [GWh]*
Re-injection of warm water from heat exchange	3.2
Re-injection of cool water from heat pumps	−11.9
Thermal inflow from warm basements	6.3
Total thermal input	−2.4

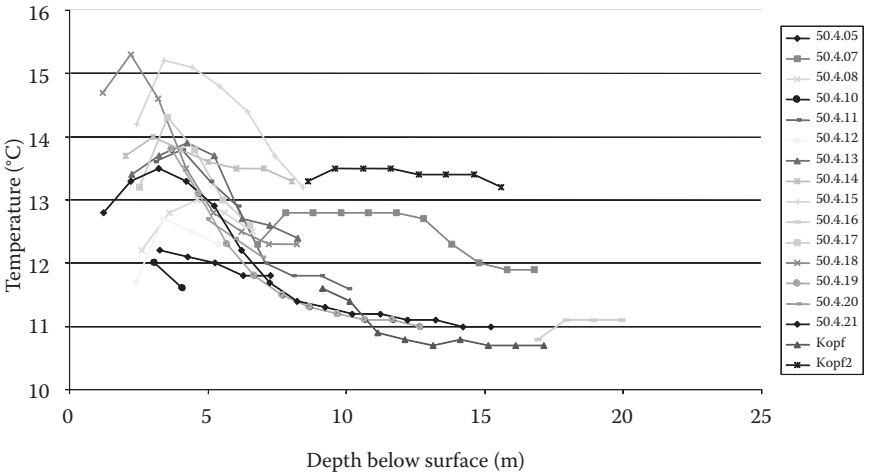

Figure 7.1 **(See color insert.)** Altach study: temperature profiles in boreholes, measured on November 13, 2001. (Modified after Cathomen, N., Wärmetransport im Grundwasser, Auswirkungen von Wärmepumpen auf die Grundwassertemperatur am Beispiel der Gemeinde Altach im Vorarlberger Rheintal. Diploma thesis, ETH Zurich, Institute of Hydromechanics and Water Resources Management, 2002.)

For the **simulation of the regional heat transport**, it was conceived that only **temperature change** ΔT, which is caused by anthropogenic influence, relative to the "natural" conditions, is relevant and thus modeled. Therefore, **heat input** is considered by the following sources:

- **Reinjection of warm water from heat exchange** for cooling purposes
- **Reinjection of cool water from heat pumps** for heating purposes
- **Thermal inflow from warm basements** of buildings

A further heat input is due to the sewer system and possibly other infrastructure devices, but those were disregarded here. The energy extraction by heat pumps is relatively well known from the licensing documents. For the injection of warm water, only the discharge was known. The related heat load was estimated as a mean temperature increase of 4 K. The heat inflow from basements was estimated using a typical basement temperature of 15°C and assuming a linear mean temperature gradient between basement and average groundwater depth, together with a typical thermal conductivity value. The area of the basements was determined from the fraction of the buildings in the settlement area. This fraction was estimated to be 10% based on the topographic map. The balance of the anthropogenic heat input is shown in Table 7.1. From the balance, it can be seen that

the estimated total heat input is negative, indicating a net cooling effect over the area.

For the simulation, the **software package** PMWIN (Chiang and Kinzelbach 2001) was used. The flow calculations were performed with the module MODFLOW96 (USGS 2012) and the **transport calculations** with module MT3DMS (Zheng and Wang 1999). The model was conceived as a two-dimensional, unconfined, one-layer model. Therefore, the variables head and temperature correspond to average values over the thickness of the aquifer. The flow model was conceived for steady-state flow conditions, thus neglecting seasonal variations of boundary conditions like inflow rates. The resulting flow velocities are therefore long-term average values. With regard to the relatively small, expected heat transport velocities of the order of 200 m year^{-1}, and the small depth to groundwater (2–3 m) and the relatively small aquifer thickness (15–20 m) in the relevant part of the model, this procedure is justified. The **hydraulic conductivity field and the lateral inflow rates** were taken from the existing and calibrated steady-state groundwater model of the International Governmental Commission of the Alpine Rhine region (IRKA). The size of the finite difference cells was 100 m. The recharge rate due to precipitation was 0.5 mm day^{-1}. This value was estimated considering the time span before the measurement campaign. Fixed head boundary conditions were set along River Rhine and Alter Rhein based on measurements. Along the northeastern boundary as well as part of the southwestern boundary, lateral inflow was prescribed based on flux estimates. Interactions with **creeks** were modeled by the leakage concept. **Head isolines** are presented in Figure 7.2. The flow in the plain area is mainly parallel to River Rhine with a typical flow gradient of about 0.002. Comparison of the calculated heads with measured data (IRKA) yielded a standard deviation of 0.5 m.

The **heat transport simulation** was performed according to the mathematical formulation presented in Chapter 4.1 for **two-dimensional aquifers**. By **utilizing the analogy between solute transport and heat transport** (Chapter 4.1.1), the transport parameters of the two-dimensional MT3DMS model were determined. As outlined above, the temperature difference $\Delta T(\mathbf{x})$ was modeled. This implies that also heat transport is considered as steady state. This was achieved using the transient transport code MT3DMS over a sufficiently long time span. The initial temperature increment $\Delta T(\mathbf{x}, t = 0)$ was set to zero. For streamline boundaries, a thermally insulating boundary was assumed. Inflow boundaries were set to zero thermal inflow boundaries. The influence of deeper sediment layers and a geothermal heat flux were neglected in the thermal model. Longitudinal dispersivity was chosen as 50 m and the transversal one as 5 m. Porosity was estimated as 0.25, λ_m as 2.7 W m^{-1} K^{-1}, C_m as 2.87×10^{-6} J m^{-3} K^{-1}, and the effective vertical thermal conductivity $\lambda_{eff,vert}$ as 1.8 W m^{-1} K^{-1}. The equivalent transport coefficients were calculated cell-wise using areal information on the land

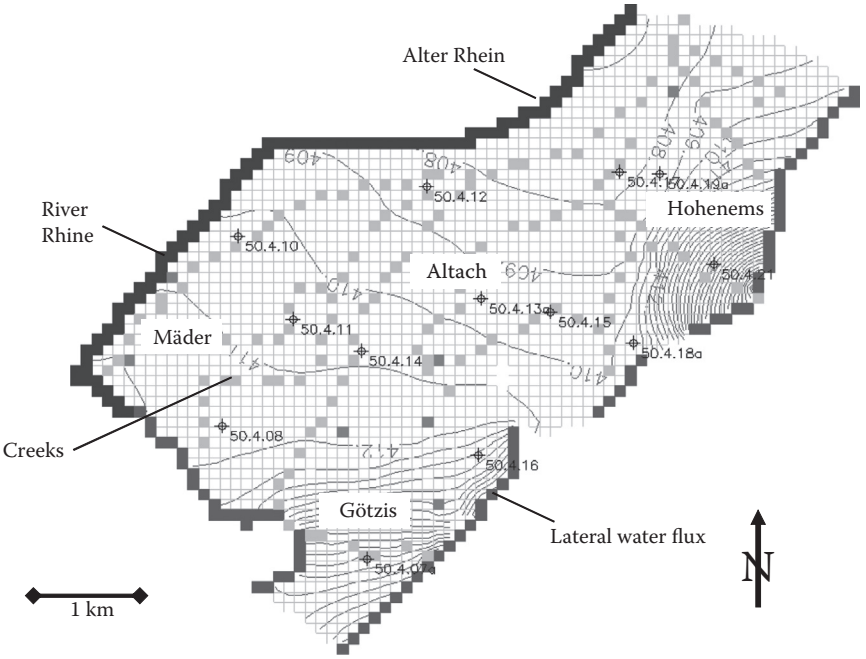

Figure 7.2 **(See color insert.)** Altach study: two-dimensional flow model Altach (Austria) with head isolines (equidistance 1 m). Dark blue: river cells; blue: prescribed inflow cells; bright blue: creeks. (Modified after Cathomen, N., Wärmetransport im Grundwasser, Auswirkungen von Wärmepumpen auf die Grundwassertemperatur am Beispiel der Gemeinde Altach im Vorarlberger Rheintal. Diploma thesis, ETH Zurich, Institute of Hydromechanics and Water Resources Management, 2002.)

use (i.e., basement) depth to groundwater, aquifer thickness, and thermal parameters of the subsurface. The areal thermal inflow from warm basements of buildings was estimated cell-wise as described above. Initial relative temperature as well as boundary conditions (lateral inflow) were set to zero everywhere.

Simulations were performed for 10 and 75 years. It was shown that the thermal plumes can be considered in quasi steady state after about 10 years. The temperature differences were calculated separately for the different thermal input cases (reinjection of warm water from heat exchange, reinjection of cold water from heat pumps, warming by basements). The reason for this procedure is that in the analogy to solute transport, the concentrations have to be positive. Therefore, all cases were calculated with positive absolute values of temperature differences separately, and the results were finally superimposed. The **resulting distribution of the relative temperature** $\Delta T(\mathbf{x})$ caused by reinjection of warm water from heat exchange, reinjection

from groundwater heat pumps, and thermal inflow from warm basements is shown in Figure 7.3.

Simulated maximum and minimum temperature changes were 3.2 and –2.6 K, respectively. Peak regions are found close to and downstream of settlements mainly. Note that warming plumes occur as often as cold plumes, and both are of similar absolute value. For the inner settlement area of the town of Altach, it was found that the temperature change was close to zero or even slightly positive. This means that the thermal input in this subregion is almost balanced. The **simulated temperature differences are compared with the measured** ones (Table 7.2). Absolute differences between both are smaller than 1 K. We have to keep in mind that the measured data

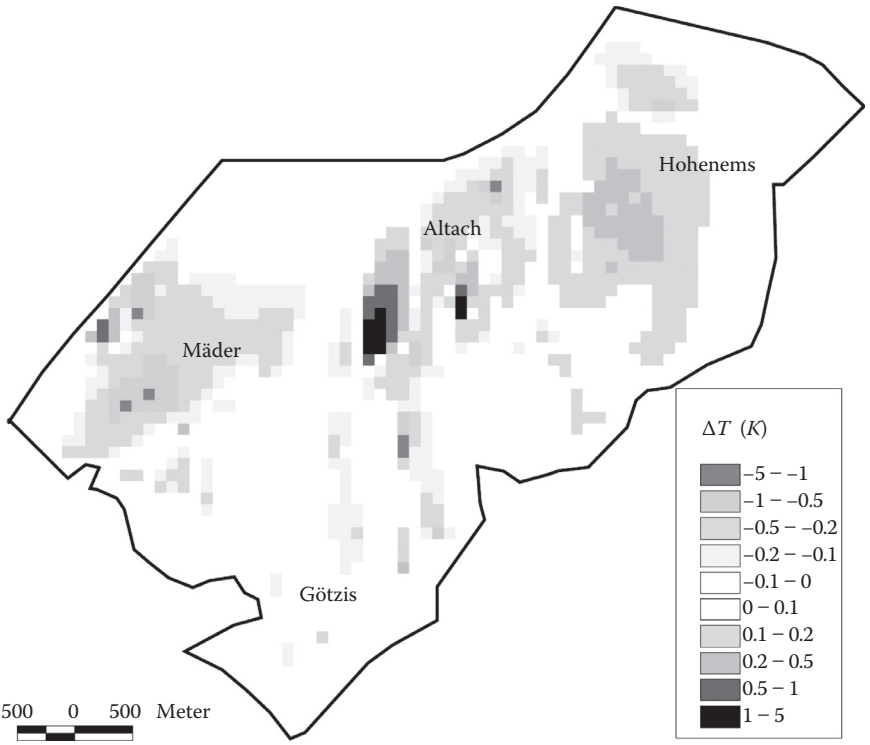

Figure 7.3 **(See color insert.)** Altach study: two-dimensional heat transport model Altach (Austria) with temperature increase due to thermal use (groundwater heat pumps, heating by constructions). Dark blue: river cells; blue: prescribed inflow cells. (Modified after Cathomen, N., Wärmetransport im Grundwasser, Auswirkungen von Wärmepumpen auf die Grundwassertemperatur am Beispiel der Gemeinde Altach im Vorarlberger Rheintal. Diploma thesis, ETH Zurich, Institute of Hydromechanics and Water Resources Management, 2002.)

Table 7.2 Altach study: measured and simulated mean temperature differences $\Delta T = T - T_{mean}$

Station	*Depth of measurement below soil surface (m)*	*Measured mean temperature difference (K)*	*Simulated mean temperature difference (K)*
50.4.11	4.85	+0.70	−0.2
50.4.13	4.33	−0.26	+0.0
50.4.21	3.20	+0.81	+0.1
50.4.17	3.92	−0.85	+0.2
50.4.20	5.90	+0.24	−0.1
Average		+0.47	+0.0

are measured 1 m below the deepest groundwater table level. Therefore, the measurements do not necessarily represent average profile temperatures exactly. Nevertheless, it can be concluded that the model simulates the mean temperatures with an accuracy of about 0.5 K. The inaccuracy includes the effect of variable soil surface temperature over the area.

7.2 LIMMAT VALLEY AQUIFER ZURICH (SWITZERLAND)

The Limmat Valley aquifer extends from the downtown area of the city of **Zurich** (Switzerland) and River Sihl along River Limmat over a distance of about 16 km with a mean and maximum width of about 1 to 2 km. The total area is about 20 km^2 comprising the part with aquifer thickness larger than 2 m. It is a highly conductive, unconfined, sandy gravel aquifer. The Limmat Valley was formed in its main disposition in the early Pleistocene (Kempf et al. 1986). The main erosion of the U-shaped valley occurred during the Riss ice age. The sediment filling occurred mainly in the Würm ice age with several stages of the glaciation and related forming of moraines and fluvial deposits. Therefore, the structure of the aquifer is quite complex and consists of sand, gravel deposits, lake sediments, and moraine material. The contributing rivers are River Limmat, starting downtown Zurich at the lake of Zurich, and the smaller River Sihl, which extends from the perialpine region to its confluence with River Limmat. Land surface topography ranges between 380 and 410 m a.s.l.

River Sihl is infiltrating into the aquifer via unsaturated percolation with a mean annual temperature of 10.7°C–11.3°C (period 2000–2003). However, the expected infiltration rates are relatively small. On the other hand, infiltration from **River Limmat** is more significant. It occurs along the major part of the river section mostly directly into the aquifer, in parts

via unsaturated percolation. The corresponding **annual temperature** is 10.2°C–11.3°C (period 2000–2003). River water infiltration influences the seasonal temperature regime considerably, with its amplitude decreasing with distance from the river. In the downtown area, mean groundwater temperatures range between 12.1°C and 16.5°C (Jäckli 2010). **How can the increase in the groundwater temperature due to anthropogenic influence roughly be assessed?** Based on the annual air temperature of the station Zurich-Affoltern of 9.6°C–10.3°C (period 2000–2003, data MeteoSwiss) and the soil surface temperature of 11.3°C–11.9°C with a mean value of 11.5°C, the mean difference between the air and soil temperature amounts to 1.2–1.7 K with a mean value of 1.5 K. Adopting roughly the temperature difference between soil surface and noninfluenced groundwater (outside the range of infiltrating rivers), the temperature increase due to anthropogenic reasons is therefore between about 0.5 and 5 K, which is the same range as reported in German cities (Menberg et al. 2013). This estimated anthropogenic increase depends mainly on the density of warm basements and the depth to groundwater. Outside the downtown region of Zurich, the anthropogenic influence is expected to be smaller. Nevertheless, a typical temperature increase of 2–3 K in urban areas is also postulated by the groundwater agency of the Canton of Zurich (AWEL 2005). This represents a considerable additional potential for thermal use, besides the allowed temperature change of 3 K according to the Swiss regulations. Systematic, long-term groundwater temperature monitoring does not yet exist for the Limmat Valley aquifer but is planned for the future (AWEL 2005). Note that the temperature of River Limmat is slightly higher than the estimated soil surface temperature and that River Sihl is clearly cooler.

The authorities of the Canton of Zurich were relatively reluctant in the past with respect to the promotion of the thermal use of groundwater. Nevertheless, about 100 installations have been approved. As a rule, the **performance of an installation** has to exceed 150 kW in order to ensure improved quality standards in maintenance. For the future, an increase in the thermal use of groundwater is expected.

In the context of master projects at the Institute of Environmental Engineering, ETH Zurich, **groundwater temperature profiles** of 47 piezometers in the Limmat Valley aquifer were measured on April 14, 2005. They show the vertical temperature profiles typical for the season and the influence of the infiltration of river water. Maximum temperatures were mainly found at greater depth. These values, lying outside of the influence of river water infiltration, can be considered as indicators of the mean groundwater temperature. In the downtown area, these values range between 12.2°C and 14.6°C, thus similar to the data of Jäckli (2010).

For various sections of the Limmat Valley aquifer, **two-dimensional groundwater flow and heat transport modeling** was performed. The method and codes correspond to those already described for the Altach study

(Section 7.1). For illustration, results are shown for the **region of the town of Schlieren** (Müller and Ott 2005; Figure 7.4). This town is situated downvalley from the City of Zurich. The area of the model domain was 4.7 km^2. The area comprises settlement areas (including industry) with a fraction of 60%. The rest consists of agricultural areas as well as recreational areas. The domain contains nine groundwater pumping stations for drinking and process water (total of about 6300 m^3 day^{-1}). Boundary condition types of the flow model are shown in Figure 7.4. Measured hydraulic conductivity values (2×10^{-4} to 10^{-2} m s^{-1}) were interpolated, and the recharge rate was estimated. Leakage coefficients of River Limmat and lateral inflow rates were calibrated. Comparison between calculated and measured heads (on April 14, 2005) yielded a mean standard deviation of about 0.3 m. For simplicity, it was assumed that the mean temperature of the river water corresponds to the "natural" groundwater temperature. Heat flow from basements to groundwater was calculated using Equation 4.5 with a temperature difference of 3 K with respect to the soil surface temperature and the areal fraction of buildings in the finite difference cells. The **simulated warming effect by basements alone** is shown in Figure 7.5. The results seem plausible. Direct comparison with measured data was not possible as no data were available. The **superimposed effect of two possible installations for thermal use** of a capacity of 315 and 196 kW is shown in Figure 7.6. The results indicate a

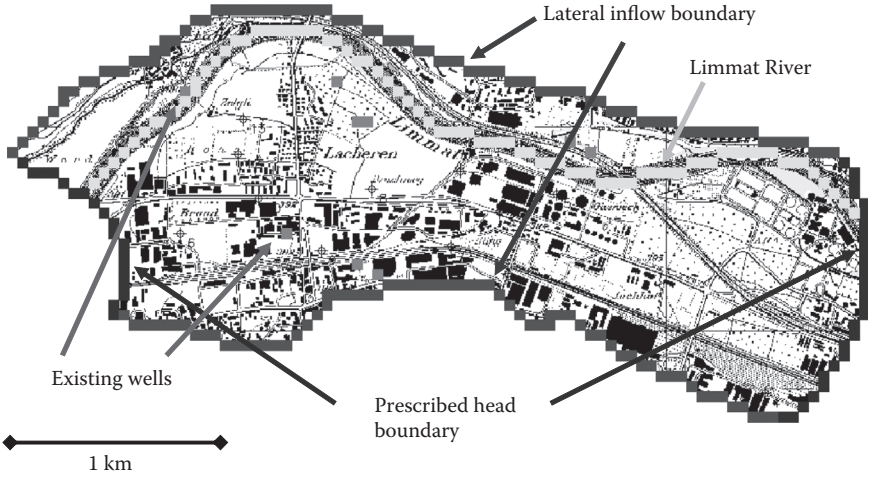

Figure 7.4 **(See color insert.)** Case study Limmat Valley, subregion town of Schlieren: model domain with wells, and boundary conditions. (Modified after Müller, E., Ott, D., Thermische Nutzung des Grundwasserleiters Limmattal, Teilgebiet Hardhof-Schlieren [Thermal use of the Limmat Valley aquifer: Area Hardhof-Dietikon]. Report Master Project, ETH Zurich, Institute of Environmental Engineering, 2005.)

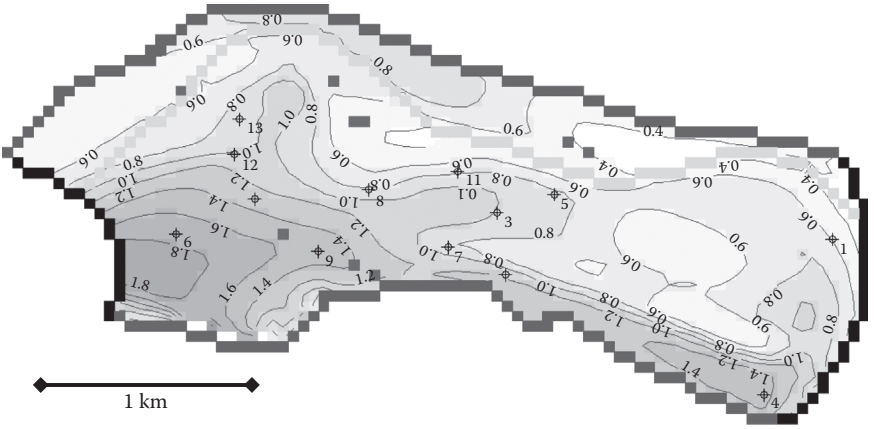

Figure 7.5 **(See color insert.)** Case study Limmat Valley, subregion town of Schlieren: quasi-steady-state simulation of the temperature increase by warm basements. (Modified after Müller, E., Ott, D., Thermische Nutzung des Grundwasserleiters Limmattal, Teilgebiet Hardhof-Schlieren [Thermal use of the Limmat Valley aquifer: Area Hardhof-Dietikon]. Report Master Project, ETH Zurich, Institute of Environmental Engineering, 2005.)

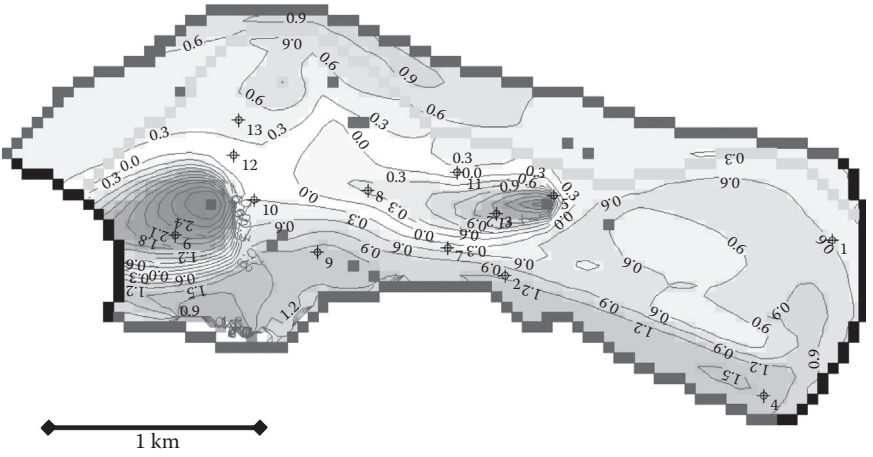

Figure 7.6 **(See color insert.)** Case study Limmat Valley, subregion town of Schlieren: quasi-steady-state simulation of the temperature increase by warm basements, and, superimposed, two planned installations for the thermal use of groundwater. (Modified after Müller, E., Ott, D., Thermische Nutzung des Grundwasserleiters Limmattal, Teilgebiet Hardhof-Schlieren [Thermal use of the Limmat Valley aquifer: Area Hardhof-Dietikon]. Report Master Project, ETH Zurich, Institute of Environmental Engineering, 2005.)

maximum temperature decrease of 4.5 K. The requirement of a maximum change in temperature downstream at a distance of 100 m according to the Swiss regulations (Chapter 1.8.1) is met for both installations. Moreover, an interference of the two installations with respect to groundwater temperature is avoided.

7.3 BAD WURZACH (GERMANY)

Only a few geothermal test sites for GSHP systems exist worldwide, which allow studying the thermal development in the subsurface in the vicinity of a borehole heat exchanger (BHE). A prominent example is the Elgg site, Switzerland, which is already mentioned in Chapter 5.1. Eugster (2001) and Rybach and Eugster (2010) monitored and simulated the long-term behavior of a BHE in a conduction-dominated system with negligible groundwater influence. The data showed that over the last years of the operation (1996–1998), the temperature stabilized showing only minor temperature changes (<1 K) in comparison to the beginning of the operation in 1986.

In the framework of the research project "geomatrix.bw," a **test site for a geothermal ground source heating pump** (GSHP) **system** was developed in **Bad Wurzach**, South Germany (Wagner and Blum 2012; Bisch et al. 2012). The main objective of the project was to monitor the temperature distribution of the near field of a BHE. However, in contrast to the study in Elgg, the examined BHE is partially **influenced by advection**. In 2009, a BHE (EW1/09) with double U-tubes and five observation wells (B0 at larger distance, B1–4 in the vicinity) were installed (Figure 7.7). Also, four coaxial systems were installed, but here we focus on the BHE with the four adjacent observation wells. The site is located south of a marshland in the Molasse basin. In the study area, the stratigraphy is characterized by Quaternary gravels, sands, and clays on top followed by clay-, marl-, and sandstones of the Upper Freshwater Molasse (UFM), which were encountered on site at 58 m depth, with a total thickness of 400–500 m. The upper part of the geological profile of the BHE (EW1/09) with a total length of 100 m based on core drilling is illustrated in Figure 7.8. The distances of the four downstream observation wells (B1, B2, B3, and B4) from the BHE are 3.9, 5.7, 7.9, and 14.1 m, respectively (Figure 7.7). The temperature sensors (Pt100) in the BHE and the observation wells were merely installed in the upper Quaternary aquifer and aquitard down to 35 m depth (Figure 7.8).

The local groundwater flow direction in the upper aquifer is generally north toward the marshland, which begins at a distance of about 400 m from the study site. Repeated and continuous groundwater level measurements showed that the groundwater flow direction fluctuates between 2° and 7° east and the groundwater level changes by a maximum of about 25 cm. The average hydraulic gradient is 0.002. In a nearby pumping well, a

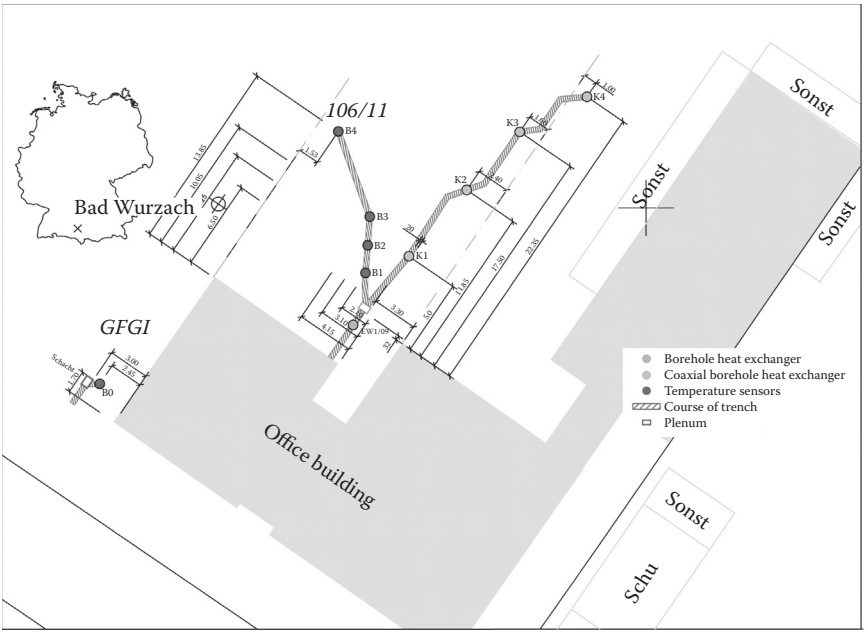

Figure 7.7 **(See color insert.)** Bad Wurzach study: site map showing the locations of the BHE (EW1/09) and the five observation wells (B0, B1, B2, B3, and B4).

long-term pumping test resulted in a hydraulic conductivity of 7×10^{-3} m s^{-1} (Table 7.3), which can be considered an average value for the heterogeneous aquifer.

Temperature monitoring in the observation wells over a time period of one year is illustrated in Figure 7.9. In winter 2011, the heating results in a minor decrease in subsurface temperatures (–1.1 K), which is more pronounced in the aquitard. However, this **thermally affected zone** (TAZ) is only visible in a distance of 3.9 m at the observation well B1. Furthermore, in summer 2011, the subsurface temperature indicates a full thermal recovery. The maximum temperature change due to the cooling and heating operation of the GSHP system was 2.9 K (7.7°C in March 2011 and 10.6°C in September 2012) at observation well B1 in 21 m depth (Bisch et al. 2013). At the observation well B4 (distance of 14.1 m), however, the maximum detected temperature change is only 0.4 K showing the limited spatial reach of the thermal disturbance around the BHE, despite the influence by a groundwater flow velocity of about 3.5 m day^{-1}.

To further study the evolution of the TAZ of the GSHP system, a 3D numerical heat transport model was set up in FEFLOW (Figure 7.10). For the latter, the input values, which are provided in Table 7.3, were used. Due to the incomplete data, a simplified layered model was implemented.

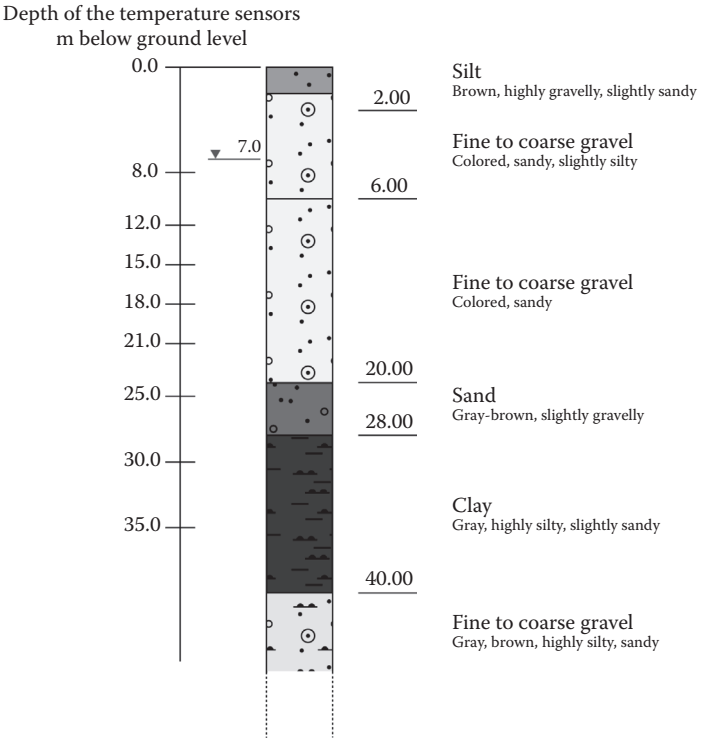

Figure 7.8 Bad Wurzach study: geological profile of the BHE (EW1/09) determined by drilling cuttings and depth of the installed temperature sensors in the observation wells B1, B2, and B3.

Table 7.3 Determined, estimated, and fitted hydraulic and thermal parameters of the geothermal test site at Bad Wurzach, Germany

Parameter	*Value*
Hydraulic conductivity, K_w (m s^{-1})	0.007[a]
Hydraulic gradient (hor.), I_{hor} (–)	0.002[b]
Porosity, ϕ (–)	0.35[c]
Longitudinal dispersivity, β_L (m)	5.0[d]
Transverse dispersivity, β_T (m)	5.0[d]
Volumetric heat capacity of the porous media, C_m [J $(m^3 K)^{-1}$] [c]	2.4×10^6
Thermal conductivity of the porous media, λ_m [W $(m K)^{-1}$]	1.4[c]

[a] Long-term pumping test at the Haidgauer Haide from 1968 (Weinszieher 1984).
[b] Hydraulic gradient based on a determined groundwater contour map (Wagner and Blum 2012).
[c] Estimated parameter value.
[d] Fitted parameter value.

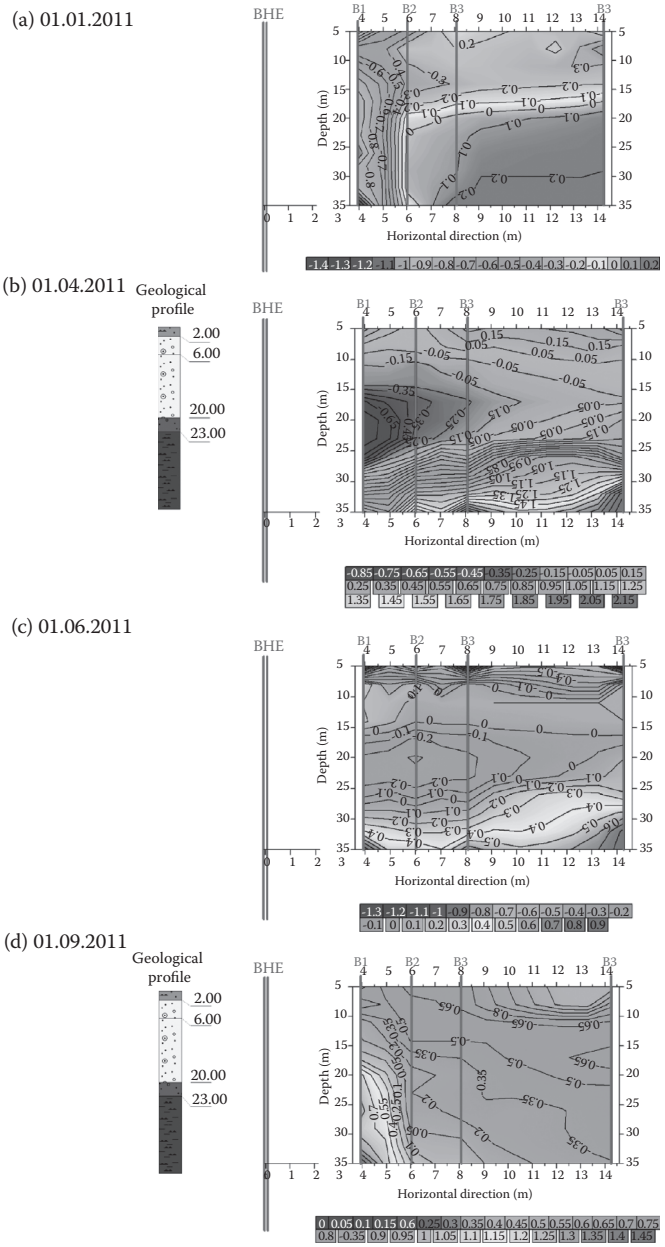

Figure 7.9 **(See color insert.)** Bad Wurzach study: cross section of the temperature measurements in various depths in groundwater flow direction over a time period of one year.

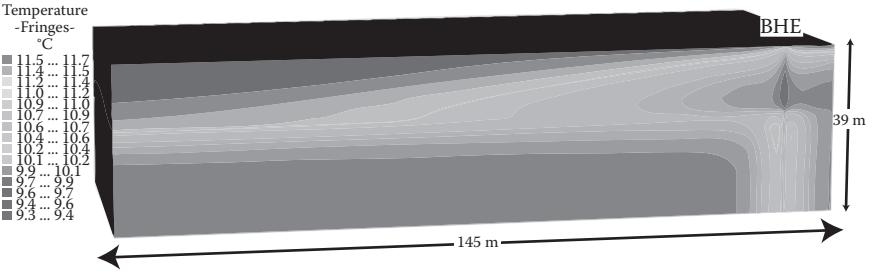

Figure 7.10 **(See color insert.)** Bad Wurzach study: 3D numerical heat transport model of the BHE (EW1/09) showing the resulting temperature plume after 160.4 days.

The time period between May 13, 2011 and December 6, 2011 (200 days) was chosen for a preliminary modeling study, because before that period, no heat meter was installed at the heat pump and therefore no detailed information on heat extraction by the BHE was available. The measured temperatures at the observation wells for the studied time period at a depth of 21 m are shown in Figure 7.11. The maximum observed temperature difference in this time period is smaller than 2.5 K in the closest observation

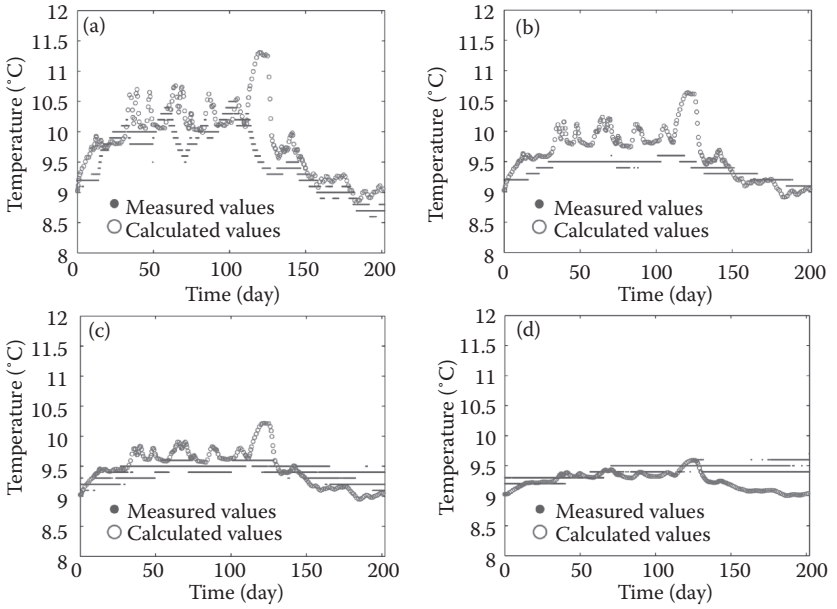

Figure 7.11 **(See color insert.)** Bad Wurzach study: comparison between measured and simulated temperatures at the four observation wells (a) B1, (b) B2, (c) B3, and (d) B4 in 21 m depth in the vicinity of the BHE (EW1/09).

well B1. The recorded temperature developments in all wells clearly show the cooling period in spring and summer, and the heating period in autumn and winter, reflected by increase and decrease in groundwater temperatures. As expected, this temperature signal is strongly damped with increasing distance from the BHE. After manual calibration of the dispersivity, the results of the preliminary numerical simulations roughly match the monitored temperatures (Figure 7.11). However, this fit could only be obtained using a relatively large dispersivity value of 5 m. This shows that hydraulic heterogeneity causes substantial macrodispersive spreading of the thermal plume. The model that assumes a homogeneous aquifer layer can only approximate these effects by specifying a large dispersivity (Table 7.3). The down-gradient observation wells show smoother temperature trends than the simulated ones, which could potentially be captured by an increasing dispersivity. Alternatively, this could also indicate an underestimation of the role of heat diffusion or temporal variability of the flow field.

Both geothermal test sites, in Elgg (Switzerland) and in Bad Wurzach (Germany), with mainly conductive or partially advective conditions, indicate that the **TAZs around BHEs** are spatially limited even after longer operation time. Hence, any planned or required temperature monitoring, for example, in the context of licensing issues by environmental authorities (Hähnlein et al. 2013), should carefully consider these circumstances.

REFERENCES

AWEL (2005). *Massnahmenplan Wasser im Einzugsgebiet Limmat und Reppisch (Planned Measures for the Catchment of Rivers Limmat and Reppisch)*. Amt für Abfall, Wasser, Energie, Luft, Kanton Zürich, Zurich, Switzerland.

Birkholzer, J.T., Tsang, Y.W. (2000). Modeling the thermal-hydrologic processes in a large-scale underground heater test in partially saturated fractured tuff. *Water Resources Research* 36(6), 1431–1447.

Bisch, G., Klaas, N., Braun, J. (2012). geomatrix.bw: Teil 3: Validierung von Erdwärmesondensimulationen zum Kühlen und Heizen im Nah- und Fernfeld mit Hilfe geothermischer Testfelder. Report ZO4E28002, Stuttgart.

Blau, R.V., Werner, A., Würsten, M., Kobus, H., Söll, T., Zobrist, J., Hufschmied, P. (1991). *Natürlicher und künstlicher Wärmeeintrag: Auswirkungen auf den Grundwasserhaushalt (Natural and Experimental Temperature Effects: Consequences on Ground Water Resources)*. Gas, Wasser, Abwasser (GWA), Schweizerischer Verein des Gas- und Wasserfaches, Zürich, Switzerland, Vol. 71, pp. 173–230, ISSN 0036-8008.

Cathomen, N. (2002). Wärmetransport im Grundwasser, Auswirkungen von Wärmepumpen auf die Grundwassertemperatur am Beispiel der Gemeinde Altach im Vorarlberger Rheintal. Diploma thesis, ETH Zurich, Institute of Hydromechanics and Water Resources Management, Zurich, Switzerland.

Cathomen, N., Stauffer, F., Kinzelbach, W., Osterkorn, F. (2002). Thermische Grundwassernutzung. Auswirkung von Wärmepumpenanlagen auf die Grundwassertemperatur. *GWA* 82(12), 901–906.

Chiang, W.-X., Kinzelbach, W. (2001). *2D Groundwater Modeling with PMWIN: A Simulation system for Modeling Flow and Transport Processes*. Springer, Berlin.

Eugster, W.J. (2001). *Langzeitverhalten der EWS-Anlage in Elgg (ZH)—Spotmessung im Herbst 2001*. Swiss Federal Office of Energy, Bern, Switzerland, 14 pp.

Hähnlein, S., Bayer, P., Ferguson, G., Blum, P. (2013). Sustainability and policy for the thermal use of shallow geothermal energy. *Energy Policy* 59, 914–925.

Jäckli. (2010). *Wohnsidlung Hardau II, Bullingerstrasse, Grundwasser-Wärmenutzung, Numerische Modellierung von bestehenden und künftigen Nutzungen im Stadtgebiet Zürich (Numerical Modeling of Existing and Future Thermal Use in the City Area of Zurich)*. Dr. Heinrich Jäckli AG, Zürich, Switzerland; Stadt Zürich, Immobilien-Bewirtschaftung, Zürich, Switzerland (unpublished).

Kempf, T., Freimoser, M., Haldimann, P., Longo, V., Müller, E., Schindler, C., Styger, G., Wyssling, L. (1986). Die Grundwasservorkommen im Kanton Zürich. Beiträge zur Geologie der Schweiz, Geotechnische Serie. Issued by: Schweiz. Geotechnische Kommission and Direktion der öffentlichen Bauten des Kantons Zürich.

Kobus, H., Söll, T. (1992). Modellierung des regionalen Wärmetransports: Fallbeispiele Kaltwassereinleitung Aefligen und Emmeinfiltration Kirchberg (Modelling of regional heat transport: Case studies coldwater discharge Aefligen and Emme infiltration Kirchberg). In: H. Kobus (Ed.), *Schadstoffe im Grundwasser, Band 1: Wärme- und Schadstofftransport im Grundwasser*. Deutsche Forschungsgemeinschaft DFG, VDH Verlagsgesellschaft mbH, Weinheim, Germany, pp. 341–375.

Kupfersberger, H. (2009). Heat transfer modeling of the Leinitzer Feld aquifer (Austria). *Environmental Earth Science* 59, 561–571.

Lo Russo, S., Civita, M.V. (2009). Open-loop heat pumps development for large buildings: A case study. *Geothermics* 38, 335–345.

Markle, J.M., Schincarion, R.A., Sass, J.H., Molson, J.M. (2006). Characterizing the two-dimensional thermal conductivity distribution in a sand and gravel aquifer. *Soil Science Society of America Journal* 70, 1281–1294.

Menberg, K., Bayer, P., Zosseder, K., Rumohr, S., Blum, P. (2013). Subsurface urban heat islands in German cities. *Science of the Total Environment* 442, 123–133.

Molson, J.W., Frind, E.O., Palmer, C.D. (1992). Thermal energy storage in an unconfined aquifer. 2. Model development, validation, and application. *Water Resources Research* 28(19), 2857–2867.

Molz, F.J., Parr, A.D., Andersen, P.F. (1981). Thermal energy storage in a confined aquifer. *Water Resources Research* 17(3), 641–645.

Molz, F.J., Warman, J.C., Jones, T.E. (1978). Aquifer storage of heated water: Part I—A field experiment. *Ground Water* 16(4), 234–241.

Müller, E., Ott, D. (2005). Thermische Nutzung des Grundwasserleiters Limmattal, Teilgebiet Hardhof-Schlieren (Thermal useofthe Limmat Valleyaquifer: Area Hardhof-Dietikon). Report Master project, ETH Zurich, Institute of Environmental Engineering, Zurich, Switzerland.

Nam, Y., Ooka, R. (2010). Numerical simulation of ground heat and water transfer for groundwater heat pump system based on real-scale experiment. *Energy*

and Buildings 42(1), 69–75. http://journals.ohiolink.edu/ejc/article.cgi?issn=03787788&issue=v42i0001&article=69_nsoghapsbore.

ÖWAV (2009). Thermische Nutzung des Grundwassers und des Untergrunds—Heizen und Kühlen (Thermal use of groundwater and underground—Heating and cooling). ÖWAV-Regelblatt 207, Österreichischer Wasser- und Abfallwirtschaftsverbands ÖWAV (Guideline 207 of the Austrian Water and Waste Management Association), Vienna, Austria.

Palmer, C.D., Blowes, D.W., Frind, E.O., Molson, J.W. (1992). Thermal energy storage in an unconfined aquifer. *Water Resources Research* 28, 2845–2856.

Papadopulos, S.S., Larson, S.P. (1978). Aquifer storage of heated water: Part II—Numerical simulation of field results. *Ground Water* 16(4), 242–248.

Parr, A.D., Molz, F.J., Melville, J.G. (1983). Field determination of aquifer thermal energy parameters. *Ground Water* 21(1), 22–35.

Rybach, L., Eugster, W.J. (2010). Sustainability aspects of geothermal heat pump operation, with experience from Switzerland. *Geothermics* 39, 365–369.

Sass, J.H., Lachenbruch, A.H., Munroe, R.J. (1971). Thermal conductivity of rocks from measurements on fragments and its application to heat-flow determinations. *Journal of Geophysical Research* 76, 3391–3401.

Sauty, J.P., Gringarten, A.C., Fabris, H., Thiery, D., Menjoz, A. Landel, P.A. (1982b). Sensible energy storage in aquifers. 2. Field experiments and comparison with theoretical results. *Water Resources Research* 18(2), 253–265.

Sauty, J.P., Gringarten, A.C., Menjoz, A., Landel, P.A. (1982a). Sensible energy storage in aquifers. 1. Theoretical study. *Water Resources Research* 18(2), 245–252.

Söll, T. (1985). Vertikal-ebene Modellierung einer Kaltwassereinleitung in das Grundwasser. *Wasserwirtschaft* 75(9), 384–392, Springer, Berlin, SSN: 0043-0978.

Tsang, C.F., Buscheck, T., Doughty, C. (1981). Aquifer thermal energy storage: A numerical simulation of Auburn University field experiments. *Water Resources Research* 17(3), 647–658.

USGS (2012). 3D Finite-difference groundwater flow model MODFLOW. *United States Geological Service*, http://water.usgs.gov/software/lists/groundwater.

Vandenbohede, A., Hermans, T., Nguyen, F., Lebbe, L. (2011). Shallow heat injection and storage experiment: Heat transport simulation and sensitivity analysis. *Journal of Hydrology* 409, 262–272.

Wagner, V., Blum, P. (2012). geomatrix.bw: Teil 2: Prozessmodellierung und Chancenanalyse oberflächennaher Erdwärme in Baden-Württemberg. Report ZO4E28004, Karlsruhe.

Weinszieher, R. (1984). Hydrogeologische und quartärgeologische Untersuchungen im Raum Bad Waldsee-Wolfegg-Bad Wurzach (Lkr. Ravensburg, Oberschwaben). Albert-Ludwigs-Universität, Freiburg.

Xue, Y., Xie, C., Li, Q. (1990). Aquifer thermal energy storage: A numerical simulation of field experiments in China. *Water Resources Research* 26(10), 2365–2375.

Zheng, C., Wang, P.P. (1999). MT3DMS: A modular three-dimensional multi-species transport model for simulation of advection, dispersion and chemical reactions of contaminants in groundwater systems; Documentation and user's guide. U.S. Army Engineer Research and Development Center Contract Report SERDP-99-1, Vicksburg, Mississippi.